The [BMI][Tf_2N] Ionic Liquid/Water Binary System: A Molecular Dynamics Study of Phase Separation and of the Liquid−Liquid Interface

N. Sieffert and G. Wipff*

Laboratoire MSM, UMR CNRS 7177, Institut de Chimie, 4 rue B. Pascal, 67 000 Strasbourg, France

Received: March 24, 2006; In Final Form: May 3, 2006

We report molecular dynamics (MD) simulations of the aqueous interface of the hydrophobic [BMI][Tf_2N] ionic liquid (IL), composed of 1-butyl-3-methylimidazolium cations (BMI^+) and bis(trifluoromethylsulfonyl)-imide anions (Tf_2N^-). The questions of water/IL phase separation and properties of the neat interface are addressed, comparing different liquid models (TIP3P vs TIP5P water and +1.0/−1.0 vs +0.9/−0.9 charged IL ions), the Ewald vs the reaction field treatments of the long range electrostatics, and different starting conditions. With the different models, the "randomly" mixed liquids separate much more slowly (in 20 to 40 ns) than classical water−oil mixtures do (typically, in less than 1 ns), finally leading to distinct nanoscopic phases separated by an interface, as in simulations which started with a preformed interface, but the IL phase is more humid. The final state of water in the IL thus depends on the protocol and relates to IL heterogeneities and viscosity. Water mainly fluctuates in hydrophilic basins (rich in O(Tf_2N) and aromatic CH(BMI) groups), separated by more hydrophobic domains (rich in CF_3(Tf_2N) and alkyl(BMI) groups), in the form of monomers and dimers in the weakly humid IL phase, and as higher aggregates when the IL phase is more humid. There is more water in the IL than IL in water, to different extents, depending on the model. The interface is sharper and narrower (∼10 Å) than with the less hydrophobic [BMI][PF_6] IL and is overall neutral, with isotropically oriented molecules, as in the bulk phases. The results allow us to better understand the analogies and differences of aqueous interfaces with hydrophobic (but hygroscopic) ILs, compared to classical organic liquids.

Introduction

Ionic liquids (ILs) based on hydrophobic ions such as imidazolium derivatives and anions such as hexafluorophosphate (PF_6^-) or bis(trifluoromethylsulfonyl)imide (Tf_2N^-; see Figure 1) form biphasic systems with water[1,2] and can be used in separation processes.[3−8] Interestingly, liquid−liquid extraction of metallic cations to ILs using classical extractant molecules (e.g., crown ethers,[5−7] phosphoryl derivatives,[3,4] or calixarenes[8]) give higher extraction, compared to classical organic phases. Interfacial phenomena play a crucial role in such processes, as the ions (initially in water) and the extractants (initially in the IL) likely meet in this peculiar domain, but our knowledge of "what happens at the interface"[9] in ion extraction is still quite limited. In the case of classical liquids, insights can be obtained in principle from spectroscopy,[10] electrochemistry,[11] kinetic studies,[12] surface tension measurements,[13] and, theoretically, by computer simulations, mainly of molecular dynamics MD type.[14−17] In the case of ionic liquids, most studies dealt with the IL/gas interface,[18−21] and IL/water interfaces have been studied by MD simulations. Lynden-Bell et al. studied the aqueous "interface" with the water-miscible dimethylimidazolium chloride IL,[22] while our group considered the [BMI][PF_6] and [OMI][PF_6] ILs based on butyl- (BMI^+) or octylmethylimidazolium (OMI^+) cations, respectively.[23]

This paper deals with the aqueous interface of the [BMI][Tf_2N] IL, focusing on the questions of phase separation from water, the extent of IL/water mixing in the "bulk phases", and the properties of the neat interface, also addressing methodological issues such as the effect of solvent model, the treatment of Coulombic interactions, and the role of the preparation protocol. More specifically, we consider two different starting states: one where the two liquids are initially juxtaposed and form a "planar interface", and one where they are "randomly mixed" at the microscopic level (Figure 1). In the case of classical mixtures (e.g., water/chloroform), both types of configurations converged in ca. 0.5 ns to the same biphasic system,[24,25] but with the [BMI][PF_6] IL, the convergence was quite slow and still incomplete after 40 ns.[23] It is thus important to investigate how the more hydrophobic [BMI][Tf_2N] IL behaves in water mixtures.

Concerning the representation of solvents, there is so far little experience about the compatibility of water and IL models to simulate their binary mixtures.[26−28] Simulations with the [BMI][PF_6] IL have shown that the model developed for the pure IL[29,30] leads to exaggerated mixing with water and that more satisfactory results can be obtained by turning the IL more hydrophobic, i.e., by scaling down the atomic charges of the IL ions.[23] Whether this is a general requirement to simulate other ILs is unclear. This is why we will compare the $[BMI]^{1.0}[Tf_2N]^{-1.0}$ model with integer charges on the IL ions to the $[BMI]^{0.9}[Tf_2N]^{-0.9}$ model with reduced charges. Concerning water, the TIP3P model that was used in the previous simulations[23,31] is known to exaggerate the water diffusion, compared to experiment or to other models.[32] Furthermore, this model originally developed using "feathered" cutoff of electrostatics[33] may be less satisfactory when used in different conditions. Interfacial and transport properties of TIP3P water obtained with Ewald summation calculations are further from

* wipff@chimie.u-strasbg.fr.

10.1021/jp061849q CCC: $33.50
Published on Web 06/13/2006

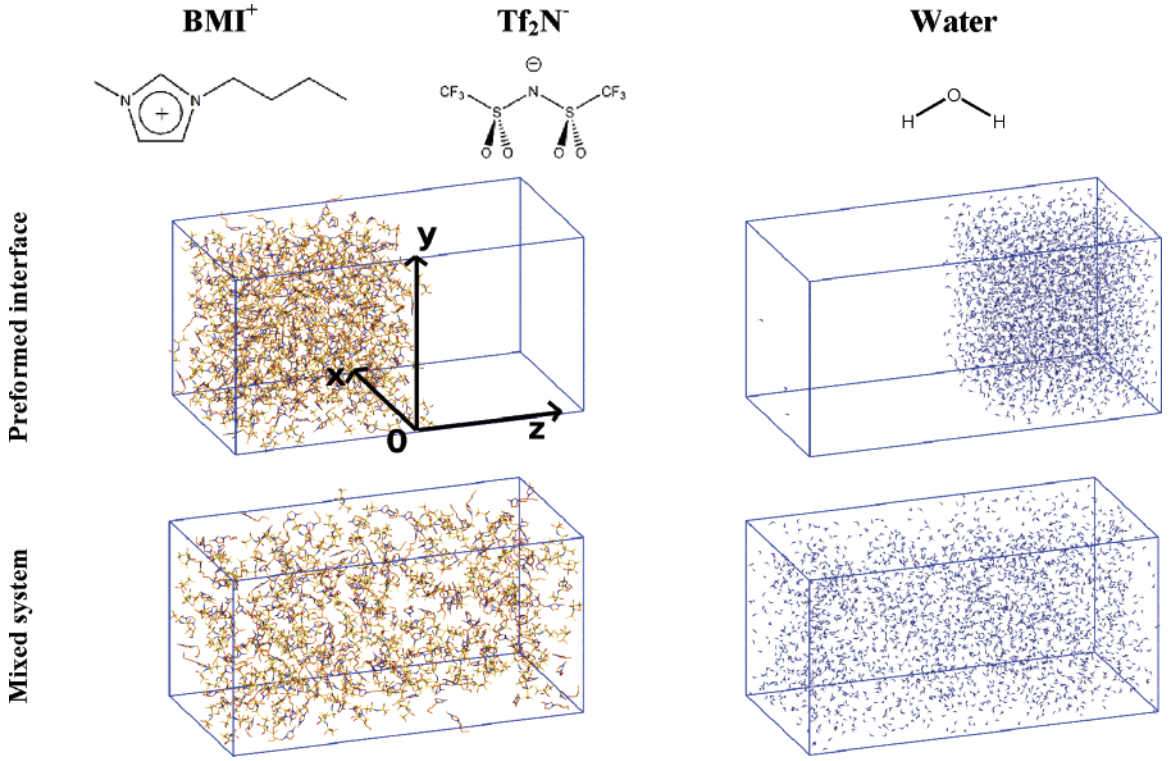

Figure 1. BMI^+ and Tf_2N^- ions and schematic representation of the IL/water interface with two starting configurations: preformed planar interface (**PL** simulations) and mixed system (**DE** simulations).

experiment than the cutoff-based results.[34] It would certainly be desirable to test solvent models involving polarization effects,[20,35] but this is presently precluded due to the long simulation times needed to equilibrate IL mixtures (vide infra). As a first approach, we decided to compare the TIP3P model to the TIP5P one which better accounts for the water diffusion.[36] Most calculations will be based on the Ewald treatment of electrostatics,[37,38] but tests with the reaction field correction[39] will also be performed. The resulting microscopic insights should allow us to better understand the analogies and differences between aqueous interfaces with hydrophobic ILs, compared to organic solvents.

Methods

Molecular Dynamics. The MD simulations were performed with the modified AMBER 7.0 software[40] where the potential energy is described by a sum of bond, angle, and dihedral deformation energies, and pairwise additive 1-6-12 (electrostatic + van der Waals) interactions between nonbonded atoms.

$$U = \sum_{\text{bonds}} K_r(r - r_{\text{eq}})^2 + \sum_{\text{angles}} K_\theta(\theta - \theta_{\text{eq}})^2 + \sum_{\text{dihedrals}} \sum_n V_n[1 + \cos(n\omega - \gamma)] + \sum_{i<j} \left[\frac{q_i q_j}{R_{ij}} - 2\epsilon_{ij}\left(\frac{R^*_{ij}}{R_{ij}}\right)^6 + \epsilon_{ij}\left(\frac{R^*_{ij}}{R_{ij}}\right)^{12} \right]$$

Cross terms in van der Waals interactions were constructed using the Lorenz−Berthelot rules. The parameters used for the $[BMI]^1[Tf_2N]^{-1}$ IL have been developed on the pure ionic liquid properties: those of BMI^+ were taken from Andrade et al.,[29] while those of Tf_2N^- were from Lopes and Padua.[41] The charges of the $[BMI]^{0.9}[Tf_2N]^{-0.9}$ IL were obtained by scaling the BMI^+ and Tf_2N^- atomic charges by a factor of 0.9, which somewhat mimics the anion to cation charge transfer[42] and renders the ions more hydrophobic. Water was described by the TIP3P[33] or TIP5P[36] model of Jorgensen et al. The 1−4 van der Waals interactions were scaled down by a factor of 2.0, and the corresponding Coulombic interactions were scaled down by 1.2, as recommended by Cornell et al.[43] The liquid systems were represented with 3D periodic boundary conditions, thus corresponding to alternating slabs of water and of the IL when they form a "flat" interface. The nonbonded interactions were calculated using a 12 Å atom-based cutoff correcting for the long-range electrostatics using the Ewald summation method (PME approximation),[37,38] and several tests were performed with the reaction field "RF" correction using a 15 Å atom-based cutoff.[39] Whereas the former method assumes a 3D periodic representation of the system and sums over all resulting charge contributions, the RF procedure assumes that the atoms within the cutoff sphere are immersed in a polarizable dielectric medium with which it interacts, leading in practice to zeroed interactions at the cutoff boundaries. A dielectric constant of 80 was taken for the continuum. Unless otherwise indicated, the MD simulations were performed at 300 K, starting with random velocities. The temperature was monitored by coupling the system to a thermal bath using the Berendsen algorithm[44] with a relaxation time of 0.2 ps. All C−H and O−H bonds were constrained with SHAKE, using the Verlet leapfrog algorithm with a time step of 2 fs to integrate the equations of motion.

The liquid−liquid "preformed" interface was built from two adjacent cubic boxes of IL and water, containing, respectively, 219 BMI^+ Tf_2N^- ion pairs and 2657 H_2O molecules (Figure 1). After 1000 steps of energy minimization, the systems were equilibrated by a sequence of (i) 50 ps of dynamics at constant volume with frozen water to relax the IL phase (BELLY option of AMBER), (ii) 100 ps of dynamics with frozen water at a

TABLE 1: Simulated Systems[a]

	solvent models	box size (Å)	electrostatics	time[b] (ns)
	[BMI][Tf_2N]−Water Binary Systems at 300 K			
PL1	$[BMI]^1[Tf_2N]^{-1}$ + TIP3P	45.0 × 45.0 × 90.1	12 Å + Ewald	20
DE1	$[BMI]^1[Tf_2N]^{-1}$ + TIP3P	45.0 × 45.0 × 90.1	12 Å + Ewald	40
PL2	$[BMI]^1[Tf_2N]^{-1}$ + TIP3P	45.0 × 45.0 × 90.1	15 Å + RF	20
DE2	$[BMI]^1[Tf_2N]^{-1}$ + TIP3P	45.0 × 45.0 × 90.1	15 Å + RF	40
PL3	$[BMI]^{0.9}[Tf_2N]^{-0.9}$ + TIP3P	45.2 × 45.2 × 90.4	12 Å + Ewald	20
DE3	$[BMI]^{0.9}[Tf_2N]^{-0.9}$ + TIP3P	45.2 × 45.2 × 90.4	12 Å + Ewald	40
PL4	$[BMI]^1[Tf_2N]^{-1}$ + TIP5P	45.8 × 45.8 × 87.0	12 Å + Ewald	20
DE4	$[BMI]^1[Tf_2N]^{-1}$ + TIP5P	45.8 × 45.8 × 87.0	12 Å + Ewald	40
	[BMI][Tf_2N]−Water Binary Systems at 323 K			
PL1′[c]	$[BMI]^1[Tf_2N]^{-1}$ + TIP3P	45.0 × 45.0 × 90.5	12 Å + Ewald	10

[a] The **DE1** to **DE4** systems (demixing simulations) are simulated with the same models as the corresponding **PL1** to **PL4** systems (planar interface between juxtaposed liquids). [b] Production time, after "equilibration" for systems **PL1** to **PL4** systems and after "mixing" for systems **DE1** to **DE4**. [c] Simulation restarted from the **PL1** trajectory at 10 ns.

constant pressure of 1 atm (iii) 50 ps of dynamics at constant volume with frozen water, and (iv) 400 ps of unconstrained dynamics at a constant pressure of 1 atm in order to fit the experimental densities. The "mixing/demixing" procedure is described in refs 23 and 24. "Randomly mixed" systems were obtained by 2 ns of MD at constant volume, using a higher temperature (500 K) with biased potentials (electrostatic interactions scaled down by a factor 100). All systems were then simulated at constant volume for 20 ns when starting from preformed interfaces and for 40 ns when starting from "mixed" systems. The MD trajectories were saved every 1 ps and analyzed using our DRAW and MDS software.[45] Typical snapshots have been redrawn with the VMD software.[46] The characteristics of the simulated systems are gathered in Table 1.

Analysis of the Trajectories. The densities of water and of the IL were calculated as a function of the *z*-coordinate in slices of $\Delta z = 0.5$ Å width (axes are defined in Figure 1), and the position of the interface ($z = 0$) was dynamically defined by the intersection of the water and IL density curves (Gibbs dividing surface). Three domains were then defined: the interfacial domain (within ±12 Å from the interface) and the "bulk" IL and "bulk" water phases (beyond 12 Å from the interface). The amount of IL in a given domain was calculated as an average of BMI^+ and Tf_2N^- contributions. The width of the interface was defined as the distance between the *z*-positions where the densities of the solvent components reach 90% of their bulk density.

In "demixing" simulations, the degree of phase separation was monitored as a function of time by the demixing index λ, which would range from 1 (fully mixed system) to 0 (perfectly separated phase): $1/\lambda = 1/N(1/d_w + 1/d_{IL})$, where d_w and d_{IL} correspond to the densities of water and of IL in the mixture, and N is a normalization factor. The simulation box was split in cubic boxes of 10 Å per side in which the densities were calculated and averaged over the different boxes.

The instantaneous values of the interface area $A(t)$ were determined by selecting the water molecules at the interface with minimal *z*-value while retaining short contacts with at least two other water molecules (O···O distances at less than 4 Å), thereby excluding extracted or isolated water molecules, and smoothing their surface-accessible surface. The diffusion coefficient D was calculated from the Einstein equation:[37] $6\,Dt = \langle |r_i(t) - r_i(0)|^2 \rangle$ over 1 ns of dynamics, selecting the solvent molecules that reside in the bulk IL domain during all that time (thus excluding those that exchange with the interface or the water phase).

Results

We first describe the outcome of phase separation simulations ("demixing", noted with the prefix **DE**), compared to the preformed "planar" interface (noted with the prefix **PL**), comparing the different models. Because of computer time limitations, only selected combinations of the models are considered. Thus, the two treatments of electrostatics will be compared for the TIP3P/$[BMI]^1[Tf_2N]^{-1}$ models of liquids, and TIP3P versus TIP5P water will be compared in conjunction with the $[BMI]^1[Tf_2N]^{-1}$ IL. Similarly, the $[BMI]^1[Tf_2N]^{-1}$ and $[BMI]^{0.9}[Tf_2N]^{-0.9}$ models of the IL will be used in conjunction with TIP3P water.

Phase Separation of [BMI][Tf_2N]/Water Mixtures and Equilibration of Juxtaposed Liquids: Testing the Convergence. *Phase Separation of Completely Mixed Liquids.* The evolution of the liquids in the demixing simulations **DE** can be estimated by looking at selected snapshots (see Figure 2 and Supporting Information Figure S1 for the **DE1** system and Figures S2−S4 for the other systems). More quantitative insights can be obtained by following the time evolution of the demixing index λ, of the potential energy U of the systems (Figures 3 and S6), and the intersolvent mixing, i.e., the number of water molecules in the "bulk" IL (Figure 4) or of IL ions in "bulk" water (Figure S7).

The first important result is that, with the different models (**DE1** to **DE4**), the [BMI][Tf_2N] IL forms at the end of the dynamics (40 ns) a distinct phase with water, delineating an interfacial domain (see Figures 2 and S5). The separation is very slow, however, compared to organic solvents, due to the slow diffusion of IL ions and solvation of IL ions by water. For instance, in the **DE1** case, some IL-rich and water-rich domains appear in about 4 ns, but even at ca. 20 ns, no well-defined "planar" interface is formed, and the potential energy U is still decreasing.

The rate of phase separation and evolution of intersolvent mixing depend on the solvent models. Phase separation is slowest with TIP3P water, as about 30−40 ns are needed to observe a plateau for $\lambda(t)$ or $U(t)$; see Figure 3. Similar trends are observed with the Ewald and RF calculations (systems **DE1** and **DE2**), indicating that the treatment of electrostatics does not critically determine the outcome of phase separation. In both cases, λ decreases down to 0.4 in about 10 ns and approaches an equilibrium value of 0.2, corresponding to well-separated phases at 40 ns. As expected, when the IL is made more hydrophobic ($[BMI]^{0.9}[Tf_2N]^{-0.9}$ model; system **DE3**), the two liquids separate faster and more efficiently: λ reaches a plateau at 0.2 in "only" 20 ns. When water is represented with the TIP5P model (**DE4** system), the phases separate somewhat faster than

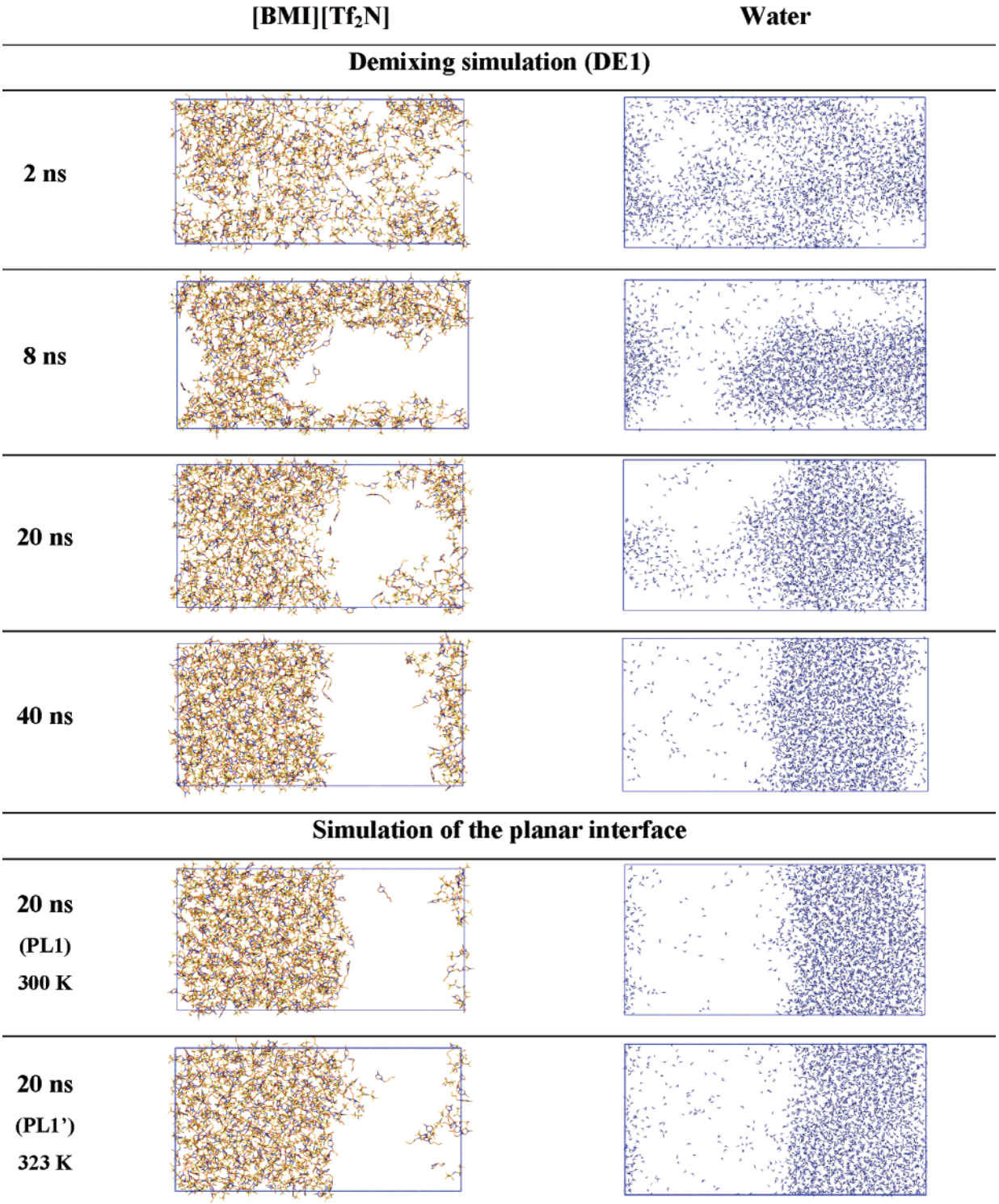

Figure 2. Simulations of the $[BMI]^1[Tf_2N]^{-1}$ IL and TIP3P water mixture: starting from completely mixed liquids (**DE1**) and from juxtaposed solvent boxes (**PL1**). Snaphots at different times, with the liquid components shown side by side for clarity.

with the TIP3P model, but the system has converged toward a different state. Indeed, after 10 ns of dynamics, it forms two alternating water slabs and IL slabs delineating four interfaces (see Figure S4). This arrangement is metastable, however, as indicated by a remixing−demixing simulation. Remixing was obtained by pursuing the dynamics for 0.32 ns at 500 K using biased electrostatics (scaled down by a factor 100). The subsequent "demixing" led to the formation of two liquid slabs only, but at the end of the simulation (40 ns), a high amount of water remained trapped as an aggregate in the IL phase. The comparison of the total potential energies of the four slabs versus two slabs containing systems (i.e., at 10 ns and 40 ns) shows that the latter is more stable, by ca. 300 ± 90 kcal/mol).

Solvent Mixing at the Preformed Interface. In the simulations of 20 ns that started from preformed interfaces, the two phases remain separated in the different tested conditions (systems **PL1** to **PL4**; see final snapshots in Figures 2 and S5). When compared to the outcome of the demixing simulations, the corresponding demixing index λ is similar (0.2), but the potential energies are lower (by 40 to 110 ± 70 kcal/mol, depending on the model; see Table S1 in Supporting Information), suggesting that they are somewhat more stable. Water gradually solu-

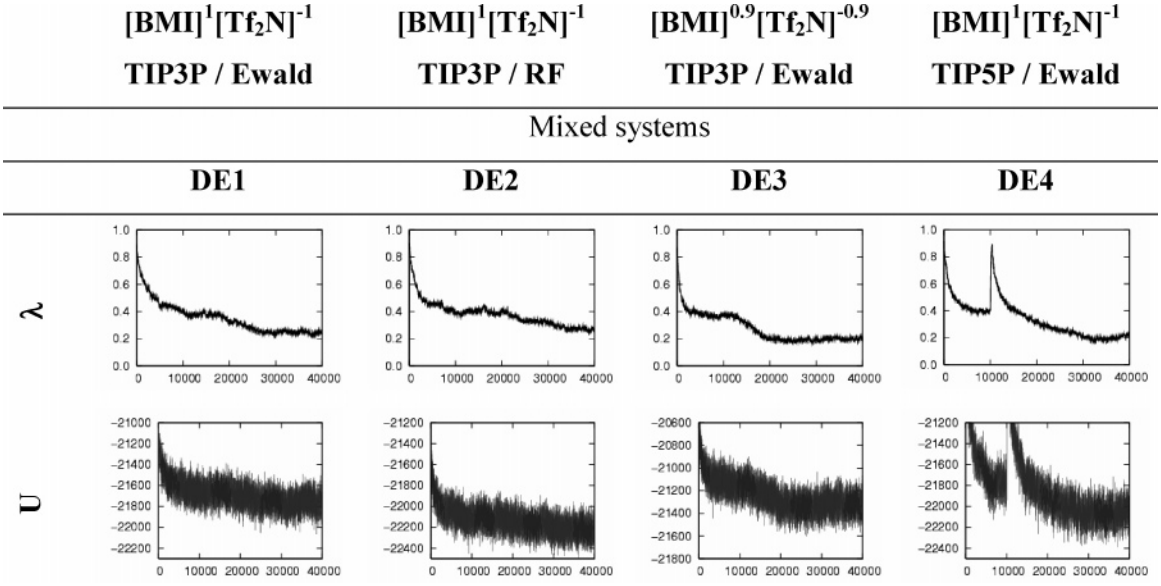

Figure 3. Evolution of the demixing index $\lambda(t)$ and of the potential energy $U(t)$ (in kcal/mol) as a function of time (in ps) in simulations which started from mixed liquids (**DE**). A full version (including the **PL** simulations) is given in Supporting Information Figure S6.

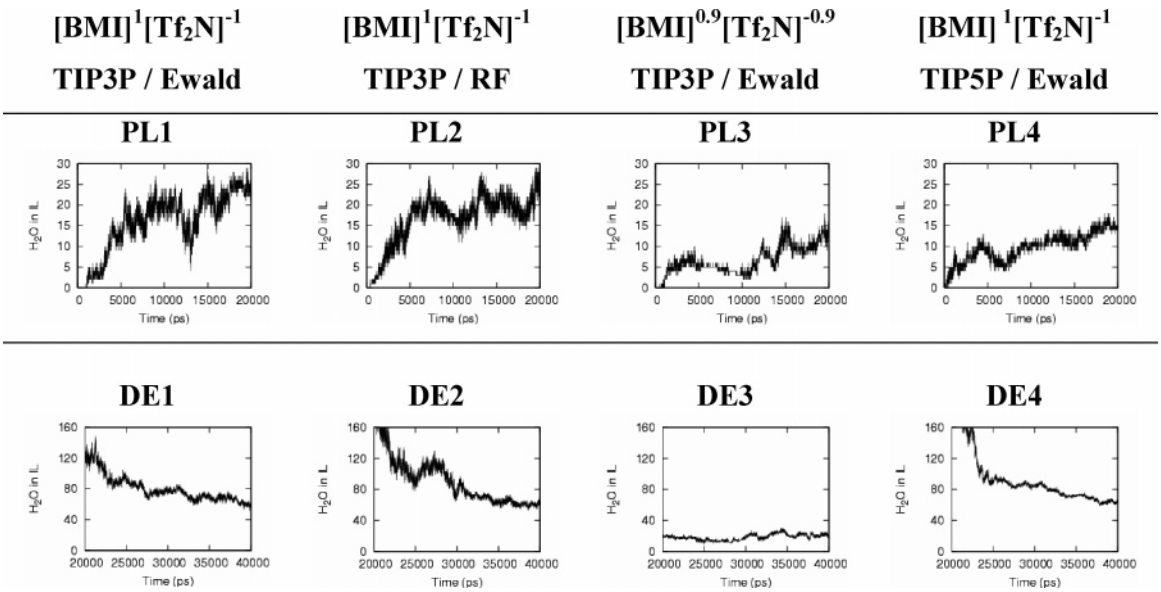

Figure 4. Number of water molecules in the bulk [BMI][Tf_2N] phase as a function of time (ps).

bilizes in the IL phase during the dynamics (Figure 4), by different amounts, depending on the solvent models. The IL humidity is not markedly influenced by the treatment of electrostatics (compare **PL1** or **PL2** systems) and is generally lower in these **PL** simulations than in the corresponding **DE** demixing simulations (Tables S2 and S3): there are ca. 25 H_2O molecules in the bulk IL phase of **PL1** or **PL2** systems and ca. 60 H_2O molecules in the **DE1** or **DE2** systems at the end of the dynamics. When the IL gets more hydrophobic ($[BMI]^{0.9}[Tf_2N]^{-0.9}$ model), the IL phase contains less water (10 H_2O in **PL3** and 20 H_2O in **DE3**) and thus less water at the preformed interfaces than in demixing simulations. The TIP5P model of water also leads to a less humid IL phase than TIP3P water does (12 H_2O in **PL4** versus 25 H_2O in **PL1**). Note that the corresponding **DE1** and **DE4** demixing simulations lead to different pictures of water in the bulk IL phases: they both contain similar amounts of water (60 H_2O molecules in **DE1** with TIP3P water versus 64 H_2O molecules in **DE4** with the TIP5P water), but TIP3P water is quite diluted, whereas TIP5P water forms big "droplets" in the IL. Considering all **PL** and **DE** simulations together, the molar fraction of water is found to range from 0.08 to 0.35 (averages over the last 0.5 ns) or from 0.07 to 0.38 (averages over the last 10 ns; see Table 2). Generally, despite the long simulated times (40 ns and 20 ns), there is no full convergence of the demixing simulations and simulations at preformed interfaces, as far as the humidity of the bulk IL phase is concerned (vide infra). This is discussed below in terms of microstructure of hydration.

On the Humidity of the IL Phase and Water State. In the literature, there are several experimental reports on the water solubility in [BMI][Tf_2N], which ranges from 0.07[47] to 0.32[48,49] in molar fraction, according to Karl Fischer titrations. Although detailed experimental protocol is sometimes lacking, we note that the lowest value has been obtained at room temperature by storing an IL solution in contact with water,[47] as well as by exposing the IL to air at 59% humidity for 24 h,[50] whereas the highest value has been obtained by stepwise addition of water to an IL solution until a distinct aqueous water phase appears and the IL humidity is constant,[48] or by contacting the IL with water for 1 h.[49] The huge discrepancy between these figures is

TABLE 2: Molar Fractions of Water in the IL ($\chi_{wat/IL}$) and of the IL in Water ($\chi_{IL/wat}$) at 300 K[a]

		$\chi_{IL/wat}$		$\chi_{wat/IL}$	
		PL	**DE**	**PL**	**DE**
1	$[BMI]^1[Tf_2N]^{-1}$/TIP3P	0.0000	0.0000	0.1739	0.3391
	Ewald	(0.0015)		(0.3657)	
		0.0005	0.0005	0.1460	0.3791
		(0.0005)		(0.3133)	
2	$[BMI]^1[Tf_2N]^{-1}$/TIP3P	0.0005	0.0000	0.1714	0.3486
	RF	0.0001	0.0002	0.1471	0.3722
3	$[BMI]^{0.9}[Tf_2N]^{-0.9}$/TIP3P	0.0000	0.0005	0.1008	0.1556
	Ewald	0.0000	0.0003	0.0714	0.1544
4	$[BMI]^1[Tf_2N]^{-1}$/TIP5P	0.0000	0.0000	0.0821	0.3462
	Ewald	0.0000	0.0001	0.0687	0.3789

[a] Averages over the last 0.5 ns of dynamics (first line) and over the last 10 ns of dynamics (second line). The values in parentheses are obtained at 323 K (**PL1′** system). The corresponding numbers of solvent molecules are given in Supporting Information Tables S2 and S3.

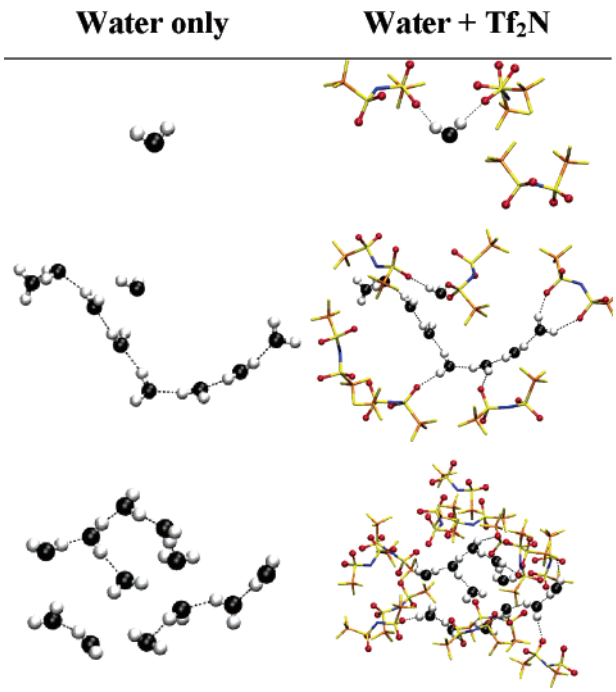

Figure 5. Typical H_2O monomer and aggregates in bulk IL (system **DE1**) shown separately (left) and with their IL surrounding ions (right). A full version of this Figure is given in Supporting Information (Figure S9).

quite surprising and hints at the existence of different states of water in the IL, depending on the experimental protocol. Which of these results should be compared to ours is unclear, but we note a qualitative agreement between both. The higher IL humidity obtained in our demixing simulations, compared to the simulations at preformed interfaces, is likely related to the microstructure of hydration, supported by the examination of the trajectories in the computer graphics. In the **PL** simulations, water generally solubilizes in the IL in the form of monomers or small oligomers (of 2−3 H_2O molecules). In the demixing **DE** simulations, one additionally finds bigger aggregates, of up to 12 H_2O molecules, forming "linear chains" or more compact assemblies inserted into polar microenvironments (Figures 5 and S8−S10). Cumulating the positions of H_2O molecules that sit in the "bulk" IL slab for 1 ns, one recognizes local "pools" where H_2O molecules diffuse and rotate, rarely exchanging, however, from one pool to the other (Figures 6 and S10). These H_2O molecules are generally hydrogen-bonded to two Tf_2N^- anions via their O(Tf_2N) oxygens and dynamically

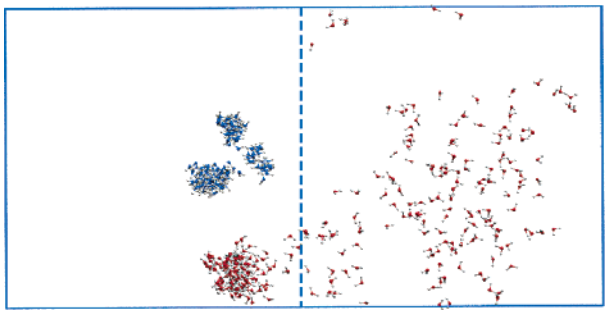

Figure 6. Diffusion of water in bulk IL (**DE1** system). Cumulated positions of two distinct H_2O molecules over the last 3 ns (every 10 ps). One H_2O (blue) oscillates between three pools in the bulk IL. The other H_2O (red) escapes from an IL pool and migrates to water. Cumulated positions of all H_2O molecule in the IL are shown in Supporting Information Figure S10.

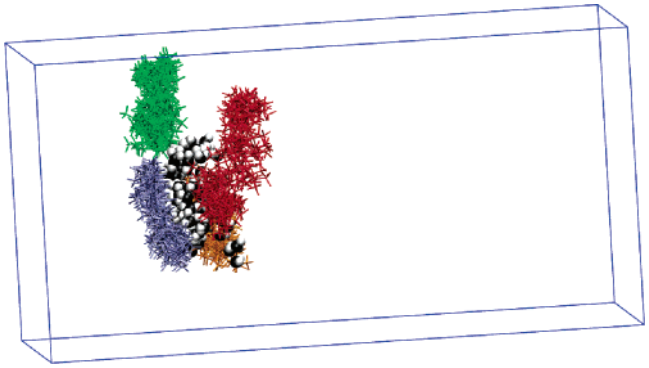

Figure 7. One H_2O molecule (oxygens in CPK black) and its four surrounding Tf_2N^- anions (in blue, red, orange, and green) in the bulk IL phase (**DE1** system). Cumulated positions during the last 10 ns.

exchange from one anion to the other within a few picoseconds. The BMI^+ cations point their CH aromatic protons toward the H_2O oxygen but make longer and weaker bonds, compared to the HO—H···(Tf_2N) bonds, which is consistent with IR spectroscopic results.[50] A typical situation is represented in Supporting Information Figure S8. Thus, the Tf_2N^- anion, although hydrophobic, may form quite strong hydrogen bonds with water.[51] On the other hand, water diffusion from one pool to the other is hampered by the crossing of more hydrophobic domains (richer in CF_3 groups and butyl(BMI^+) chains). These observations hint at a relationship between the different states of water in the IL and the local heterogeneities and dual solvation properties of the liquid.[52−55] These are also consistent with the dynamics of the IL itself which is characterized by different time scales, involving high-frequency "rattling" motions of small amplitude in local basins and much slower diffusion motions.[56−59] In some cases, the water interactions with its microenvironment may be schematically viewed as a host−guest relationship between a polar guest (water) and a "host" (IL components) possessing converging polar binding sites and diverging hydrophobic groups, thus displaying analogies with macrocyclic complexes of ions.[60] Furthermore, there is a dynamic coupling between both partners, illustrated in Figure 7, where the positions of one H_2O molecule and four surrounding Tf_2N^- anions (from the **DE1** system) are cumulated during 10 ns. The difficulty of water to escape from the "host" likely relates to the equilibration problem in computational, as well as experimental, conditions.

Solubility of IL Ions in Water. The simulations predict that the IL ions are much less soluble in water than water is in the IL. On the average, there is less than one single IL ion pair in

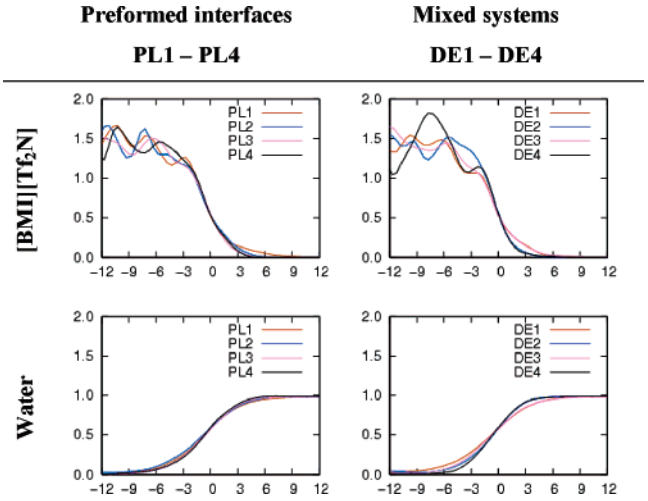

Figure 8. Density curves of the solvent in the interfacial region, as a function of the *z*-position (in Å). Averages over the last 3 ns of MD.

the simulated bulk water slab, which means that the IL molar fraction is less than 10^{-3}. Instantaneously, however, one can find a few IL ions in water, up to three BMI^+ cations and up to one Tf_2N^- anion when the most hydrophilic $[BMI]^1[Tf_2N]^{-1}$ model is used in conjunction with TIP3P water. Their occurrence as a function of time is plotted in Supporting Information Figure S7, showing a higher probability of finding BMI^+ cations over Tf_2N^- anions in water, which indicates that the anion is more hydrophobic than the cation. The results cannot thus be directly compared with the experimentally determined solubility of the IL in water (from 2.8×10^{-4} [61] to 3.2×10^{-4} [62] in molar fraction) which corresponds to a neutral solution. Calculating the average number of cations and anions in the water slab yields molar fractions smaller than 10^{-4} for the **PL3** and **PL4** systems and ranging from 10^{-4} to 5×10^{-4} for the other systems (averages over 10 ns of dynamics; see Table 2), which brackets the experimental data. Thus, a given ion is less soluble in TIP5P than in TIP3P water, and it is less soluble, as expected, when its charge is reduced from ±1 to ±0.9, i.e., from the $[BMI]^{0.9}[Tf_2N]^{-0.9}$ to the $[BMI]^1[Tf_2N]^{-1}$ IL model (see Table 2 and Figure S7).[63]

Structure and Dynamics of the [BMI][Tf$_2$N]−Water Interface. In this section, we focus on interfaces obtained from the juxtaposed liquids for consistency, but the conclusions obtained from the demixing simulations are similar.

Interface Width and Roughness. The densities of the solvents calculated during the last 3 ns of simulation are plotted as a function of the *z*-position in the simulation box (Figure 8). With the different computational models, they look quite similar in the interfacial and bulk water regions, showing that the interface is particularly sharp and narrow (∼10 Å). The main differences concern the bulk IL, whose density displays broad oscillations, in keeping with the big size of its ionic components and presence of water pools, especially in the case of the **DE4** system, as mentioned above. The different models also yield similar average values of the interface area *A* (Table S5). Note that *A* is about 2.3−3 times larger than the *XY* section of the box (which would correspond to a strictly planar interface), due to the interface roughness. Moreover, high fluctuations are observed (∼10%), underlining its dynamics character, also illustrated by snapshots of the surface of interfacial water at 0.1 ns intervals (see Figure 9 for the **PL1** system).

Ion Distribution at the Interface. The IL distribution at the interface has been investigated by averaging the number of cations and anions (defined by their center of mass) in Δ*z* slabs of 1 Å width in the simulation box. The results (Figure S11) show that the different tested models give similar ion distributions. In the bulk IL, an average of four ion pairs are found per slab, each slab being alternatively positively and negatively charged due to round-off effects. When approaching the interface, the number of ions quickly drops to zero, and no excess of anions or cations is observed at the IL side or at the aqueous side of the interface, which is therefore overall neutral. This contrasts with the [BMI][PF_6] IL whose PF_6^- anions are more hydrophilic than the Tf_2N^- anions and in excess in water, whereas the BMI^+ cations are in excess at the interface.[23]

Orientation and Conformation of the Solvent Species. The BMI^+, Tf_2N^-, and water molecules are polar and might adopt different orientations at the interface. We investigated this feature by calculating the average order parameter, defined as $S = \langle(3\cos^2\theta - 1)/2\rangle$, where θ is the angle between the *z* axis of the box and the N_1-N_2 vector of BMI^+, the S_1-S_2 vector of Tf_2N^-, or the H−H vector of the H_2O molecules (Figure S11). The *S* parameter would range from −0.5 (if the vectors were perfectly ordered parallel to the interface) to 1 (if they were perpendicular). *S* was calculated as a function of the *Z*-position of the solvent molecules, and the resulting distribution (Figure S11) shows that it oscillates around zero, indicating isotropic distributions of both solvent ions and water, in the bulk phases as well as at the interface.

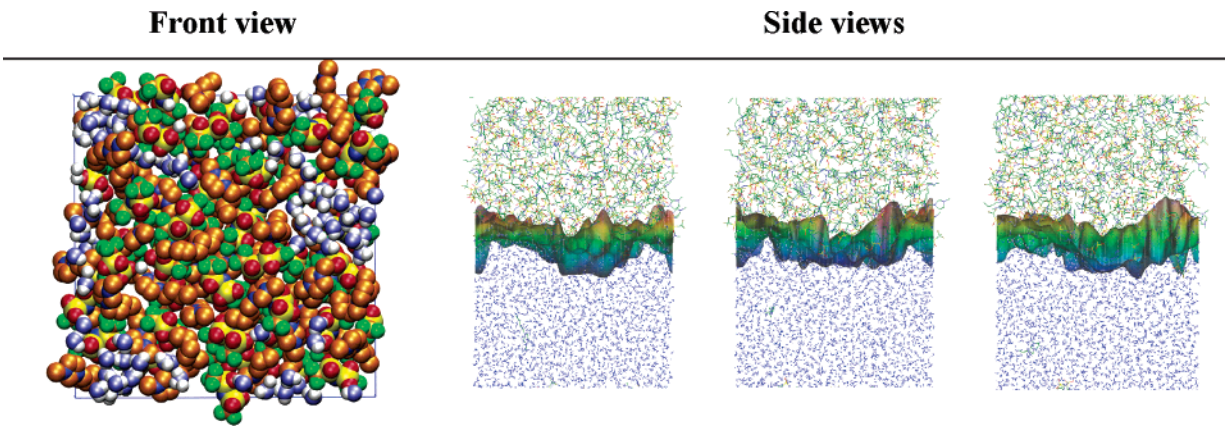

Figure 9. Snapshots of the [BMI][Tf_2N]−water interface. Left : Solvent slab of 20 Å thickness centered at the interface seen from the water side (C atoms colored in orange, N in dark blue, S in yellow, F in green, H in white, O_{Tf_2N} in red, and O_{wat} in light blue). Right: Water surface at the interface at times $t = 19.8$, 19.9, and 20.0 ns. The surface is color-coded as a function of the *z*-position, between −9 Å and +9 Å from the interface. The IL phase is above and the water phase is below the interface.

TABLE 3: Average Diffusion Coefficients in Bulk IL (10^{-7} cm^2/s) of the Solvent Molecules[a]

	1 [BMI]^1[Tf$_2$N]$^{-1}$ TIP3P/Ewald	2 [BMI]^1[Tf$_2$N]$^{-1}$ TIP3P/RF	3 [BMI]$^{0.9}$[Tf$_2$N]$^{-0.9}$ TIP3P/Ewald	4 [BMI]^1[Tf$_2$N]$^{-1}$ TIP5P/Ewald
		Planar Interfaces (**PL**)		
H_2O	6.2 ± 3.9 [18]	5.7 ± 6.1 [8]	11.2 ± 12.3 [6]	3.7 ± 4.0 [11]
BMI^+	3.5 ± 1.3 [101]	1.7 ± 0.7 [101]	4.5 ± 1.9 [93]	1.7 ± 0.8 [101]
Tf_2N^-	3.4 ± 1.2 [101]	1.8 ± 0.8 [103]	4.3 ± 1.9 [98]	1.6 ± 0.8 [103]
		Mixed Systems (**DE**)		
H_2O	8.0 ± 7.2 [36]	6.6 ± 7.7 [35]	15.5 ± 18.2 [10]	22.0 ± 28.7 [50]
BMI^+	3.3 ± 1.7 [90]	2.8 ± 1.5 [95]	2.8 ± 2.0 [93]	2.5 ± 1.4 [97]
Tf_2N^-	2.9 ± 1.3 [85]	2.7 ± 1.4 [96]	2.3 ± 1.3 [95]	2.7 ± 1.3 [103]

[a] The number of corresponding solvent molecules is given in brackets. A histogram presentation of the results is given in Supporting Information Figures S15−S17.

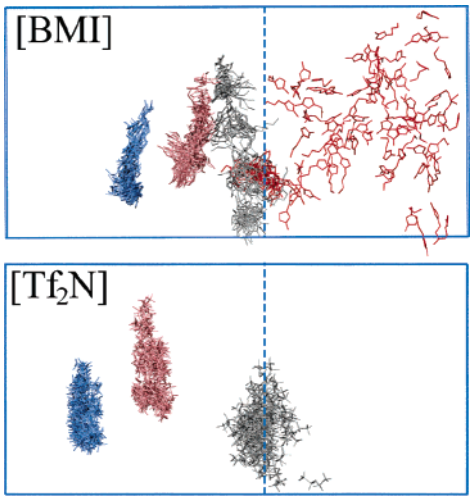

Figure 10. Diffusion of IL ions (**PL1** system). Cumulated views of four selected BMI^+ cations (top) and of three Tf_2N^- anions (bottom) over the last 10 ns (every 0.1 ns).

The above results are consistent with the view of the IL surface, seen from the water side (Figure 9), which appears as a mixture of the N and C atoms of BMI^+ cations and of F and O atoms of the Tf_2N^- anions. The N atom of Tf_2N^- is however "buried" and does not contribute significantly to the surface.

The Tf_2N^- anions and BMI^+ cations are conformationally labile but do not adopt specific conformations at the interface. Indeed, the $F_3C{-}S{\cdots}S{-}CF_3$ dihedral ϕ of a given interfacial anion exchanges between gauche$^+$ and gauche$^-$ forms during the dynamics (Figure S12). Furthermore, the statistics of ϕ also peaks around about ±70° in the bulk IL, on the aqueous side, and on the IL side of the interface (Figure S13), showing that the anions behave similarly in the different portions of the solution. Comparisons with other data can be found in refs 41, 64, 65. The butyl chain of the BMI^+ cations is also flexible, and its conformation was characterized by its overall extension (defined by the $N_{butyl}{\cdots}CH_3$ distance) whose distributions in the interfacial and bulk IL regions are plotted in Figure S14. With the different models, the distributions peak at 5.05 and 4.55 Å, which corresponds to trans−trans and gauche−trans or trans−gauche arrangements of the NC−CC and CC−CC dihedrals. There is thus no clear conformational preference of the BMI^+ cations at the interface, compared to the bulk IL.

Ionic Liquid Dynamics. In the IL domain, the BMI^+ and Tf_2N^- ions diffuse slowly, in keeping with the high viscosity of the liquid. For instance, in the case of the **PL1** system, the cumulated positions of ions selected in the bulk IL show overall translations of ca. 10−20 Å only during 10 ns (Figure 10).

Furthermore, the cations and the anions are more mobile at the interface than in bulk IL, as observed at the analogous [BMI][PF_6] interface.[23] This is also consistent with water-induced accelerated ion diffusion in ILs.[66] The case of a BMI^+ cation exchanging between the interface and the water phase is also represented in Figure 10, showing that the cation moves more rapidly in water than in the bulk IL. No such exchange could be observed for Tf_2N^- anions. More quantitative insights can be obtained by the diffusion coefficients D calculated in the bulk IL and reported in Table 3. Note that these coefficients are calculated for a small number of solvent species and with high fluctuations, in the order of magnitude of D. Histograms of D with the contributions of the different species (Figures S15−S17) give a more detailed picture of individual solvent molecules dynamics and reflect the heterogeneity and micro-diversity of the IL phase. With the four studied models, however, the cation and anion of the IL have similar D coefficients that are 2−3 times smaller that the water diffusion coefficient and comparable to the experimentally determined values (3.0×10^{-7} cm^2 s^{-1} for BMI^+ and 2.4×10^{-7} cm^2 s^{-1} for Tf_2N^- at 300 K).[67] The water D coefficients in the IL phase are about 2 orders of magnitude smaller than in pure water.[68] They are somewhat higher in the demixing **DE** than in the "planar" **PL** systems, in keeping with the higher humidity of the former IL, especially in the **DE4** system, which contains the biggest water pool. Water diffusion is also higher with the ±0.9 than for the ±1 charged IL ions, i.e., when the hydrogen bonds with the ionic liquid get weaker.

Discussion and Conclusions

We report MD investigations on the aqueous interface with the hydrophobic [BMI][Tf_2N] ionic liquid that is widely used for liquid−liquid extraction purposes, comparing the TIP3P to the TIP5P water models, and an IL model developed for the neat IL to a less polar model. With the different tested combinations of models, the randomly mixed liquids separate, leading to two phases linked by a well-defined interface, showing that, as in the case of classical water−organic solvent mixtures, neither the solvent models nor the treatment of long-range electrostatics are crucial for that process. This contrasts with the results obtained with the less hydrophobic [BMI][PF_6] IL whose representation with a "primitive model" (±1 charged ions) in conjunction with TIP3P water led to exaggerated intersolvent mixing, without forming an interface.[23] At the quantitative level, the extent of intersolvent mixing depends on the model and decreases when the IL ions get less charged or from the TIP3P to the TIP5P water model. On the other hand, comparison of the Ewald versus reaction field treatments of Coulombic interactions does not reveal marked differences at planar interface nor in demixing simulations.

More surprising is the lack of full convergence of simulations that started from equilibrated juxtaposed liquids and from mixed liquids, despite the rather long simulated times (20 ns and 40

ns, respectively). We believe that this is a specific feature of ILs related to their glassy behavior and microheterogeneity, yielding to different humidities depending on their "history" (e.g., temperature of preparation, protocol of mixing and equilibration). In some cases (e.g., TIP5P water), phase separation led to metastable lamellar-type systems, with alternating slabs of IL and water, instead of two well-defined microphases. Even in the case of "full" separation, some water remained trapped inside the IL, whose anions locally may delineate hydrophilic microbasins via their (S)O oxygens. Furthermore, hydrogen bonding to these anions is stereochemically demanding,[51] and the latter possess an "amphiphilic" constitution, thereby "repelling" water via their CF_3 groups in the interbasin regions. Thus, water hardly diffuses from one basin to the other or to the bulk water phase which should be, however, energetically favorable. We believe that this may explain the difficulty of experimentally equilibrating water in ionic liquids such as [BMI][Tf_2N], with possible aging effects. For instance, the interfacial tension of the biphasic [BMI][Tf_2N]/water system has been reported to decrease from 15.9 to 13.7 dyne cm^{-1} after several hours when the two purified liquids were put in contact, illustrating the slow diffusion and equilibration processes.[61] In the case of Eu^{3+} solvation in ILs, EXAFS studies suggested that the systems were not equilibrated after 2 days, due to the very slow kinetics.[69] The lack of convergence in the simulations at preformed interface, compared to demixing simulations, although dealing with much smaller time scales and "mesoscopic solutions", is qualitatively consistent with these observations.

Experimentally, the water solubility in a given IL depends on the temperature,[67] and interestingly, in one study giving the highest humidity, we note that the IL was first conditioned at 323 K prior being saturated with water.[48] This led us to pursue the **PL1** simulation at the interface at 10 ns for another 10 ns at 323 K (**PL1′** system), instead of 300 K. The results (Figures 2 and S18 and Table 3) show that the amount of water in the IL increases rapidly and stabilizes in ca. 5 ns, as do the λ index and the potential energy *U*. From 300 to 323 K, the calculated molar fraction of water increases from 0.17 to 0.37 (averages over the last 10 ns) or from 0.15 to 0.31 (averages over the last 0.5 ns), and interestingly, the values at 323 K are close to the experimentally reported value of 0.32. With the other solvent models, it should be somewhat smaller.

When compared to classical organic liquids used for solvent extraction purposes, ILs are more hygroscopic and partition differently in the aqueous phase. Here, some excess of BMI^+ over Tf_2N^- ions is found in bulk water with the different models, which contrasts with the case of the [OMI][PF_6] and [BMI][PF_6] ILs whose anions are less hydrophobic and in excess on the aqueous side of the interface.[23] This finding is consistent with a cation exchange mechanism in ion extraction with BMI^+-containing ILs.[5,8,70] The IL/water interface is narrower and sharper with Tf_2N^- than with PF_6^- anions[23] and does not involve local intersolvent mixing, as all solvent molecules of a given liquid retain the contact with their bulk phase, as in the case of classical organic liquids. A major difference with the latter, however, concerns the polar and "amphiphilic" nature of the IL ions, which better solvate ionic solutes that can be hydrophilic (e.g., electrolytes with hard ions) or more hydrophobic (e.g., ion complexes in ion extraction or charged reaction intermediates in phase transfer catalysis),[1,71,72] thereby facilitating their migration from the interface to the IL phase. Simulations along these lines are underway in our group.

Acknowledgment. The authors are grateful to IDRIS, CINES, Université Louis Pasteur, and GDR-PARIS for computer resources and to A. Chaumont, E. Engler, and R. Schurhammer for assistance.

Supporting Information Available: Potential energies of the systems and energy analysis of water interactions with IL ions (Tables S1 and S4). Analysis of IL/water mixing (Tables S2, S3, and Figure S7). Characteristics of the interfacial area (Table S5). Snapshots of IL and water in demixing simulations (Figures S1−S4) and at the end of the dynamics (Figure S5), and corresponding potential energies and demixing index (Figure S6). Interactions of IL with water (Figures S8−S10). Orientations and conformations at the interface (Figures S11−S14). Distribution of diffusion coefficients (Figures S15−S17). This material is available free of charge via the Internet at http://pubs.acs.org.

References and Notes

(1) Wasserscheid, P.; Welton, T. *Ionic Liquids in Synthesis*; Wiley-VCH: Weinheim, 2002.
(2) Rogers, R. D.; Seddon, K. R. *Science* **2003**, *302*, 792−793.
(3) Visser, A. E.; Jensen, M. P.; Laszak, I.; Nash, K. L.; Choppin, G. R.; Rogers, R. D. *Inorg. Chem.* **2003**, *42*, 2197−2199.
(4) Cocalia, V. A.; Jensen, M. P.; Holbrey, J. D.; Spear, S. K.; Stepinski, D. C.; Rogers, R. D. *J. Chem. Soc., Dalton Trans.* **2005**, 1966−1971.
(5) Visser, A. E.; Swatloski, R. P.; Reichert, W. M.; Griffin, S. T.; Rogers, R. D. *Ind. Eng. Chem. Res.* **2000**, *39*, 3596−3604.
(6) Chun, S.; Dzyuba, S. V.; Bartsch, R. A. *Anal. Chem.* **2001**, *73*, 3737−3741.
(7) Dai, S.; Ju, Y. H.; Barnes, C. E. *J. Chem. Soc., Dalton Trans.* **1999**, 1201−1202.
(8) Luo, H. M.; Dai, S.; Bonnesen, P. V.; Buchanan, A. C.; Holbrey, J. D.; Bridges, N. J.; Rogers, R. D. *Anal. Chem.* **2004**, *76*, 3078−3083.
(9) Watarai, H. *Trends Anal. Chem.* **1993**, *12*, 313−318.
(10) Conboy, J. C.; Richmond, G. L. *J. Phys. Chem. B* **1997**, *101*, 983−990.
(11) Girault, H. H.; Schiffrin, D. J. In *Electroanalytical Chemistry*; Bard, A. J., Ed.; Dekker: New York, 1989; Vol. 15, pp 1−141 and references therein.
(12) Danesi, P. R.; Chiarizia, R.; Coleman, C. F. In *Critical Reviews in Analytical Chemistry*; Campbell, B., Ed.; CRC Press: Boca Raton, Florida, 1980; Vol. 10, p 1.
(13) Szymanowski, J. *Solvent Extr. Ion Exch.* **2000**, *18*, 729−751.
(14) Benjamin, I. *Acc. Chem. Res.* **1995**, *28*, 233−239 and references therein.
(15) Chang, T. M.; Dang, L. X. *Chem. Rev.* **2006**, *106*, 1305−1322.
(16) Wipff, G.; Lauterbach, M. *Supramol. Chem.* **1995**, *6*, 187−207.
(17) Coupez, B.; Boehme, C.; Wipff, G. *J. Phys. Chem. B* **2003**, *107*, 9484−9490.
(18) Halka, V.; Tsekov, T.; Freyland, W. *Phys. Chem. Chem. Phys.* **2005**, *7*, 2038−2043.
(19) Rivera-Rubero, S.; Baldelli, S. *J. Am. Chem. Soc.* **2004**, *126*, 11788−11789.
(20) Yan, T.; Li, S.; Jiang, W.; Gao, X.; Xiang, B.; Voth, G. A. *J. Phys. Chem. B* **2006**, *110*, 1800−1806.
(21) Lynden-Bell, R. M.; Del Popolo, M. *Phys. Chem. Chem. Phys.* **2006**, *8*, 949−954.
(22) Lynden-Bell, R. M.; Kohanoff, J.; Del Popolo, M. G. *Faraday Discuss.* **2005**, *129*, 57−67.
(23) Chaumont, A.; Schurhammer, R.; Wipff, G. *J. Phys. Chem. B* **2005**, *109*, 18964−18973.
(24) Muzet, N.; Engler, E.; Wipff, G. *J. Phys. Chem. B* **1998**, *102*, 10772−10788.
(25) Baaden, M.; Schurhammer, R.; Wipff, G. *J. Phys. Chem. B* **2002**, *106*, 434−441.
(26) Hanke, C. G.; Lynden-Bell, R. M. *J. Phys. Chem. B* **2003**, *107*, 10873−10878.
(27) Lynden-Bell, R. M.; Atamas, N. A.; Vasilyuk, A.; Hanke, C. G. *Mol. Phys.* **2002**, *100*, 3225−3229.
(28) Shah, J. K.; Maginn, E. J. *J. Phys. Chem. B* **2005**, *109*, 10395−10405.
(29) de Andrade, J.; Boes, E. S.; Stassen, H. *J. Phys. Chem. B* **2002**, *106*, 13344−13351.
(30) Chaumont, A.; Engler, E.; Wipff, G. *Inorg. Chem.* **2003**, *42*, 5348−5356.
(31) Vayssiere, P.; Chaumont, A.; Wipff, G. *Phys. Chem. Chem. Phys.* **2005**, *7*, 124−135.
(32) Mahoney, M. W.; Jorgensen, W. L. *J. Chem. Phys.* **2001**, *114*, 363−366.

(33) Jorgensen, W. L.; Chandrasekhar, J.; Madura, J. D.; Impey, R. W.; Klein, M. L. *J. Chem. Phys.* **1983**, *79*, 926.
(34) Feller, S. E.; Pastor, R. W.; Rojnuckarin, A.; Bogusz, S.; Brooks, B. R. *J. Phys. Chem.* **1996**, *100*, 17011−17020.
(35) Dang, L. X.; Chang, T. M. *J. Chem. Phys.* **1997**, *106*, 8149−8159.
(36) Mahoney, M. W.; Jorgensen, W. L. *J. Chem. Phys.* **2000**, *112*, 8910−8922.
(37) Allen, M. P.; Tildesley, D. J. *Computer Simulation of Liquids*; Clarendon Press: Oxford, 1987.
(38) Darden, T.; York, D.; Pedersen, L. *J. Chem. Phys.* **1993**, *98*, 10089−10092.
(39) Hünenberger, P. H.; van Gunsteren, W. F. *J. Chem. Phys.* **1998**, *108*, 6117−6134.
(40) Case, D. A.; Pearlman, D. A.; Caldwell, J. W.; Cheatham, T. E., III; Wang, J.; Ross, W. S.; Simmerling, C. L.; Darden, T. A.; Merz, K. M.; Stanton, R. V.; Cheng, A. L.; Vincent, J. J.; Crowley, M.; Tsui, V.; Gohlke, H.; Radmer, R. J.; Duan, Y.; Pitera, J.; Massova, I.; Seibel, G. L.; Singh, U. C.; Weiner, P. K.; Kollman, P. A. AMBER7; University of California: San Fransisco, 2002.
(41) Canongia Lopes, J. N. A.; Padua, A. A. H. *J. Phys. Chem. B* **2004**, *108*, 16893−16898.
(42) Morrow, T. I.; Maginn, E. J. *J. Phys. Chem. B* **2002**, *106*, 12807−12813.
(43) Cornell, W. D.; Cieplak, P.; Bayly, C. I.; Gould, I. R.; Merz, K. M., Jr.; Ferguson, D. M.; Spellmeyer, D. C.; Fox, T.; Caldwell, J. W.; Kollman, P. A. *J. Am. Chem. Soc.* **1995**, *117*, 5179.
(44) Berendsen, H. J. C.; Postma, J. P. M.; van Gunsteren, W. F.; DiNola, A.; Haak, J. R. *J. Chem. Phys.* **1984**, *81*, 3684.
(45) Engler, E.; Wipff, G. In *Crystallography of Supramolecular Compounds*; Tsoucaris, G., Atwood, J. L., Lipkowski, J., Eds.; Kluwer Academic Publishers: Dordrecht, 1996; Vol. 480, pp 471−476.
(46) Humphrey, W.; Dalke, A.; Schulten, K. *J. Mol. Graphics* **1996**, *14*, 33.
(47) Huddleston, J. G.; Visser, A. E.; Reichert, W. M.; Willauer, H. D.; Broker, G. A.; Rogers, R. D. *Green Chem.* **2001**, *3*, 156−164.
(48) Jacquemin, J.; Husson, P.; Padua, A. A. H.; Majer, V. *Green Chem.* **2006**, *8*, 172−180.
(49) Luo, H.; Dai, S.; Bonnesen, P. V.; Haverlock, T. J.; Moyer, B. A.; Buchanan, A. C., III *Solvent Extr. Ion Exch.* **2006**, *24*, 19−31.
(50) Cammarata, L.; Kazarian, S. G.; Salter, P. A.; Welton, T. *Phys. Chem. Chem. Phys.* **2001**, *3*, 5192−5200.
(51) The interaction energy between Tf_2N^- and HOH amounts to −10.5 kcal/mol, according to QM calculations at the DFT/6-31G* level with BSSE correction. This is comparable to the interaction of H_2O with a PF_6^- anion, or with a BMI^+ cation (9−10 kcal/mol; see Chaumont, A.; Schurhammer, R.; Wipff, G. *J. Phys. Chem. B* **2005**, *109*, 18964−18973).
(52) Schröder, U.; Wadhawan, J. D.; Compton, R. G.; Marken, F.; Suarez, P. A. Z.; Consorti, C. S.; de Souza, R. F.; Dupont, J. *New J. Chem.* **2000**, *24*, 1009−1015.
(53) Wang, Y.; Voth, G. A. *J. Am. Chem. Soc.* **2005**, *127*, 12192−12193.
(54) Canongia Lopes, J. N. A.; Padua, A. A. H. *J. Phys. Chem. B* **2006**, *110*, 3330−3335.
(55) Chaumont, A.; Wipff, G. *J. Mol. Liq.* In press.
(56) Del Popolo, M.; Voth, G. A. *J. Phys. Chem. B* **2004**, *108*, 1744−1752.
(57) Urahata, S. M.; Ribeiro, M. C. C. *J. Chem. Phys.* **2005**, *122*, 024511−024119.
(58) Hanke, C. G.; Price, S. L.; Lynden-Bell, R. M. *Mol. Phys.* **2001**, *99*, 801−809.
(59) Margulis, C. J.; Stern, H. A.; Berne, B. J. *J. Phys. Chem. B* **2002**, *106*, 12017−12021.
(60) Lehn, J. M. *Supramolecular Chemistry, Concepts and Perpectives*; VCH: Weinheim, 1995.
(61) Toh, S. L. I.; McFarlane, J.; Tsouris, C.; DePaoli, D. W.; Luo, H.; Dai, S. *Solvent Extr. Ion Exch.* **2006**, *24*, 33−36.
(62) Shvedene, N. V.; Borovskaya, S. V.; Sviridov, V. V.; Ismailova, E. R.; Pletnev, I. V. *Anal. Bioanal. Chem.* **2005**, *381*, 427−430.
(63) Insights into interactions of IL components with water were obtained by simulating a single BMI^+ or Tf_2N^- ion in a cubic solvent box of TIP3P or TIP5P water. The analysis (see Table S4 in Supporting Information) shows that Tf_2N^- interacts more strongly with water than BMI^+ does (by ∼30 kcal/mol with the TIP3P water and by ∼10 kcal/mol with the TIP5P water). Thus, the higher hydrophobicity of the anion, compared to the cation, stems from other contributions, like the solvent−solvent interactions, involving entropic and enthalpic contributions. Comparing a given ion in TIP3P versus TIP5P water shows different trends: BMI^+ prefers TIP5P water (by 9 kcal/mol), whereas Tf_2N^- prefers TIP3P water (by 15 kcal/mol). The sum of the two ions contributions is however comparable in both solvent models (−176 vs −172 ± 7 kcal/mol).
(64) The lack of *trans* forms in our MD results stems from using a dividing factor SCEE of 1.2 for the 1−4 electrostatic interactions (recommended by Cornell et al.[43] in the AMBER force field and de Andrade et al.[29] for BMI^+) instead of 2.0 (recommended by Lopez et al. for Tf_2N^-).[41] In fact, according to QM optimizations, the *trans* form is preferred over the *gauche* form, by $\Delta E = 1.2$ kcal/mol at the DFT-B3LP/6-31G* level, and by 0.8 kcal/mol at the DFT-B3LYP/cc-pVTZ level. Repeating the AMBER calculations with SCEE = 2.0 yields better agreement with the QM values ($\Delta E = 0.7$ kcal/mol) than with SCEE = 1.2 ($\Delta E = -2.7$ kcal/mol) in the gas phase. Furthermore, pursuing the dynamics at the $IL^{\pm 1}$/TIP3P interface for 10 additional ns yields a higher population of *trans* form in the IL slab (70%) than at the interface (40%), showing that the Tf_2N^- conformation may be perturbed by its solvent environment. As indicated by X-ray structures, it also depends on the nature of the IL imidazolium cation's substituents in the solid state (see Holbrey, J. D.; Reichert, W. M.; Rogers, R. D. *Dalton Trans.* **2004**, 2267−2271). Using the SCEE of 2.0, instead of 1.2 does not change, however, our conclusions concerning the lack of preferred orientation of Tf_2N^- at the interface or the state of water in the IL.
(65) Sieffert, N.; Wipff, G. *J. Phys. Chem. A* **2006**, *110*, 1106−1117.
(66) Schröder, U.; Wadhawan, J. D.; Compton, R. G.; Marken, F.; Suarez, P. A. Z.; Consorti, C. S.; de Souza, R. F.; Dupont, J. *New J. Chem.* **2000**, *24*, 1009−1015.
(67) Tokuda, H.; Hayamizu, K.; Ishii, K.; Abu Bin Hasan Susan, M.; Watanabe, M. *J. Phys. Chem. B* **2004**, *108*, 16593−16600.
(68) Rick, S. W. *J. Chem. Phys.* **2004**, *120*, 6085−6093.
(69) Gaillard, C.; Billard, I.; Chaumont, A.; Mekki, S.; Ouadi, A.; Denecke, M.; Moutiers, G.; Wipff, G. *Inorg. Chem.* **2005**, *44*, 8335−8367.
(70) Dietz, M. L.; Dzielawa, J. A.; Jensen, M. P.; Beitz, J. V.; Borkowski, M. In *Ionic Liquids IIIB: Fundamentals, Progress, Challenges and Opportunities: Transformations and Processes*; American Chemical Society: Washington, DC, 2005; Vol. 902, pp 2−18.
(71) Chauvin, Y.; Mussmann, L.; Olivier, H. *Angew. Chem., Int. Ed. Engl.* **1995**, *34*, 2698−2700.
(72) Dupont, J.; de Souza, R. F.; Suarez, P. A. Z. *Chem. Rev.* **2002**, *102*, 3667−3691.